CHEMICAL ENGINEERING TRANSACTIONS
VOL. 110, 2024
A publication of AIDIC
The Italian Association of Chemical Engineering
Online at www.cetjournal.it
Guest Editors: Marco Bravi, Antonio Marzocchella, Giuseppe Caputo

**ISBN** 979-12-81206-10-6; **ISSN** 2283-9216
DOI: 10.3303/CET24110049

# Foam Characterization and Disruption in a Gas Sparged Pilot Stirred Tank

Niccolò Mandolini, Federico Alberini, Francesco Maluta, Giuseppina Montante, Alessandro Paglianti*

Dipartimento di Chimica Industriale "Toso Montanari", Alma Mater Studiorum – Università di Bologna, via Piero Gobetti 85, 40129 Bologna, Italy
alessandro.paglianti@unibo.it

Foaming in bioreactors can lead to severe operational problems and it is often controlled by chemical antifoam agents which cause additional downstream separation requirement and, in some cases, the decrease of gas-liquid mass transfer. For this reason, mechanical foam disruption is a very attractive alternative to chemical agents, but it is rarely adopted in industrial practice. In this work, the applicability of an agitation method for foam disruption in a gas-liquid stirred tank is considered. The stirred tank is a pilot scale version of typical industrial fermenters used in fed batch mode, with a large free volume between the upper impeller and the vessel top. The experimental characterization consists in the measurements of the local gas volume fraction, the power consumption, and the bubble size distribution in an aerated liquid with typical physical properties of fermentation broths, in different air flow rates and impeller speeds. The discussion of the results leads to a novel methodology for the foaming systems monitoring and to a strategy to control the foam by using mechanical agitation, widening the applicability of stirring as foam disruption in industrial bioreactors.

## 1. Introduction

Foam is often an issue in industrial operations requiring mechanical agitation for the dispersion of a gas phase in liquids containing surfactants, such as in fermentations and many other chemical and food processes (Leuner et al., 2020). Foam definition is not unique, but it is most often described as a gas-liquid dispersion with a very high gas volume fraction, leading to bubbles in the foam to be located on top rather than within the liquid phase (Junket, 2007). Excessive foam leads to severe issues including reduction of productivity and contamination (Varley et al., 2004). Being quite difficult to control and to predict, foam is often mitigated by chemicals. Chemical antifoams induce foam breakage due to bubble coalescence, but they also provoke side effects, such as the reduction of mass transfer surface area and the requirement of product purification (Hoeks et al., 1997). As an alternative to chemical antifoam agents, mechanical foam disruption by agitation has several advantages and it has been proved to be effective up to the industrial scale, provided that appropriate design of the impeller is selected (Boon et al., 2002). In some cases, such as for viscous foams, a combination of chemical and mechanical methods might be required (Jiang et al., 2020). Investigations on stirring as foam disruption methods date back to the 90's, leading to progresses on scale-up (Hoeks et al., 2003).
Overall, mechanical methods are still much less adopted with respect to chemical antifoam agents most likely due to the lack of comprehensive methodologies for predicting their performances. Generally, with the currently available experimental and computational methods, such as Particle Image Velocimetry (Montante et al., 2013), widely adopted for the characterization of bioreactors (Montante and Paglianti, 2015), and Computational Fluid Dynamics possibly coupled with Population Balance Models (Falzone et al., 2018), which help in the bioreactor design (Maniscalco et al., 2021), the capability to investigate and predict foaming is quite limited.
In this work, the foam entrainment capability of a stirrer as foam disruptor (SAFD) is assessed by a detailed characterization of a foaming gas-liquid stirred tank, based on strain gauge, Electrical Resistance Tomography and Laser Diffraction techniques.

Paper Received: 11 March 2024; Revised: 8 April 2024; Accepted: 12 May 2024
Please cite this article as: Mandolini N., Alberini F., Maluta F., Montante G., Paglianti A., 2024, Foam Characterization and Disruption in a Gas Sparged Pilot Stirred Tank, Chemical Engineering Transactions, 110, 289-294 DOI:10.3303/CET24110049

## 2. Experimental

A combination of techniques was used to characterize the gas-liquid dispersion, which are shortly described in the following together with the stirred tank geometry and the fluids properties.

### 2.1 The gas-liquid stirred tank

The investigated stirred tank, schematically depicted in Figure 1, consisted of a cylindrical vessel of diameter, T, equal to 0.48 m and height, H, equal to 1.7 m, equipped with four equally spaced baffles of width, W, equal to T/10. Agitation was provided with two identical Rushton turbines of diameter, D, equal to 0.19 m (D=0.40T), with the lower one set at a clearance from the flat tank bottom, $C_1$, equal to 0.24 m ($C_1$=T/2) and the second at a distance equal to T from the first ($C_2$=0.72m, $C_2$/T=1.5). The ungassed liquid height was always set at 0.79 m, that is 70mm above the upper impeller disk. Three impeller speeds, N, (200, 250 and 315 rpm) and two gas flow rates, $Q_G$, (50 and 120 L/min) were selected, resulting in six investigated conditions. The liquid was a dilute solution of 0.5 g/L Carboxymethyl cellulose (CMC) and of a 0.1 g/L nonionic polyoxyethylene surfactant (Triton X-100) in demineralized water. The resulting Newtonian solution had viscosity of 8 mPa·s, density of 991 kg/m$^3$ and surface tension of 37 mN/m at the room temperature of 20°C. Air was injected in the liquid through 36 equally spaced holes of 2 mm in diameter located on the top of a ring sparger of external diameter, $D_s$, equal to 0.1 m (Ds=0.52D) located at clearance with respect to the vessel bottom, $C_s$, equal to 85 mm ($C_s$ =0.18T). The measurements were carried out at room temperature and pressure.
Preliminary observations of the gas-liquid dispersion revealed a significant foam formation, with the foam reaching the vessel top after few minutes of agitation. To address the foam mitigation by a mechanical method, a stirrer as foam disruptor (SAFD) was mounted on top of the two RTs. The SAFD consisted of an impeller of diameter equal to 0.37 m equipped with 6 inclined blades and located at 0.142 m from the tank bottom. Most of the experiments were performed with the SAFD working in up-pumping mode, a limited analysis was performed considering the down-pumping mode. The different pumping modes were obtained reversing the rotation direction.

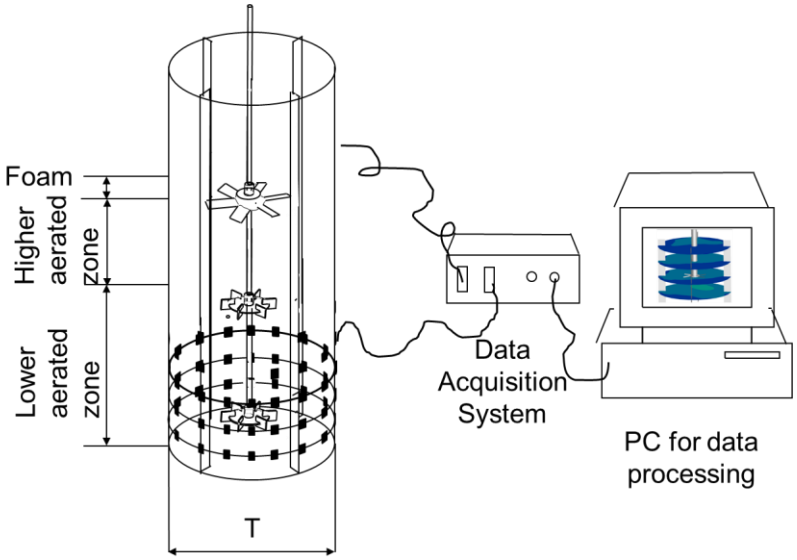


*Figure 1: Sketch of the stirred tank and of the instrumentation.*

### 2.2 Measurements techniques

The local gas hold-up distribution was determined, on three horizontal planes provided with 16 equally spaced electrodes each, by the Electrical Resistance Tomography (ERT) instrumentation P2000 (Industrial Tomography Systems Ltd.). The electrodes were squared stainless steel plates of 30 mm side and 1 mm thickness, fixed to the vessel wall, equally spaced along the vessel periphery at three axial elevations from the vessel bottom, one located below ($z_1$=0.375T) and the other two located between the two impellers ($z_2$=0.625T; $z_3$=0.875T). Additional details of the experimental techniques are omitted for the sake of brevity and they can be found elsewhere (Carletti et al., 2018).
The local dimensionless conductivity was obtained as the ratio between the conductivity measured at the selected impeller speeds and gas flow rates and the reference conductivity, measured as the average of 20 instantaneous frames collected in the ungassed liquid stirred at very low impeller speed (N=50 rpm). The local

values of the gas hold-up, which will be presented in the results, are estimated from the dimensionless conductivity obtained from the average of 100 instantaneous measurements by the application of the well-known Maxwell equation (Khalili et al., 2017) in the case of the non-conducting dispersed phase.
The overall gas hold-up was also estimated from the increase of the aerated liquid level with respect to the ungassed conditions. The liquid level variation was obtained by reading the level on a ruler attached to the external vessel wall.
The torque on the shaft was measured by using the Kistler torque sensor type 4502A020RAU, which is based on a strain gauges system. The sensor was mounted below the electrical motor, between the motor head and the metal shaft combining the two parts with couplings and adapters. It has a rated torque of 20 Nm, a maximum torque of 1.5 the rated one and an accuracy class of 0.2. At the steady state conditions, the torque and the impeller speed were measured simultaneously at the frequency of 10Hz for 3600 seconds and the power consumption was obtained from the mean of 36000 instantaneous values. For each rotational speed, a preliminary measurement of the torque due to friction dissipation was performed with the rotating shaft in the empty vessel. The power transferred by the shaft to the fluid through the impeller, P, was calculated as the net torque (measured torque minus the friction torque) times the impeller speed.
The bubble size was measured by means of a Spraytec laser diffraction system (Malvern Panalytical) equipped with a wet sample dispersion unit. The Spraytec laser diffraction system measures the intensity of light scattered as a laser beam passes through the gas-liquid dispersion. The sampling was performed after 50 minutes from the gas injection, to make sure that the system was at the steady state. About 1 L of mixture was withdrawn from the vessel and passed through the measuring cell of the Spraytec. The bubble distribution was obtained as the average of 500 measurements performed on 500 seconds. The draining point was midway between two consecutive baffles at an axial elevation of 0.47 m from the vessel bottom.

## 3. Results and discussion

The experimental investigation was guided from the visual observation of the gas-liquid stirred tank, which suggested to qualitatively describe the vessel volume as divided in three regions (named as foam, higher aerated zone, and lower aerated zone), schematically depicted in Figure 1. With the classical dual impeller configuration without SAFD, the foam always reached the vessel top quickly after the gas injection. With the SAFD mounted on the shaft, at the impeller speed N=250rpm and above with both the gas flow rates, the mechanical action was sufficient to disrupt the foam both in the up-pumping and in the down-pumping mode. Instead, at the lower impeller speed of N=200rpm, only the up-pumping rotation ensured an effective foam entrainment and disruption action. For this reason, the quantitative characterization of the system reported in the following is relevant to the up-pumping operation only.
Being the operative cost one of the SAFD limitations, the power consumption was investigated first. The time trace of the measured torque shown in Figure 2(a) provides a quantitative indication of the time required to achieve the steady state, which establishes when the aerated liquid reaches the final level close to the SAFD. The steady state power consumption reported in Figure 2(b) increases of about four times in the investigated range of impeller speeds and it is equal with the two gas flow rates, since the SAFD action leads to the same gas hold-up, as observed from the overall gas hold-up measurements based on the increase of the aerated liquid level (not shown for space constrains).

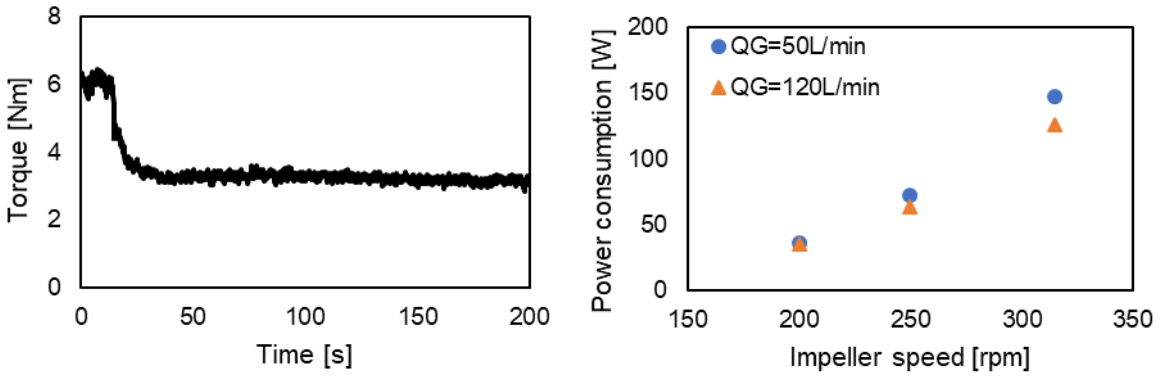


*(a)* *(b)*

*Figure 2: Time trace of the torque at $Q_G$=50L/min e N=200rpm (a) and effect of the impeller speed on the power consumption (b).*

Further insight into the system behaviour can be gained from the analysis of the gas volume fraction distribution on the three ERT planes shown in Figure 3 at three selected conditions. In all cases, the gas volume fraction does not achieve uniform distribution, but a significant improvement of the homogeneity along the vessel height is apparent at the impeller speed of 315rpm (Figure 3b), while in the other two conditions below the lower impeller the gas bubbles are definitely scant. The results suggest that the foam formation does not ensure optimal gas distribution, despite the very tiny bubble size typical of foaming systems.

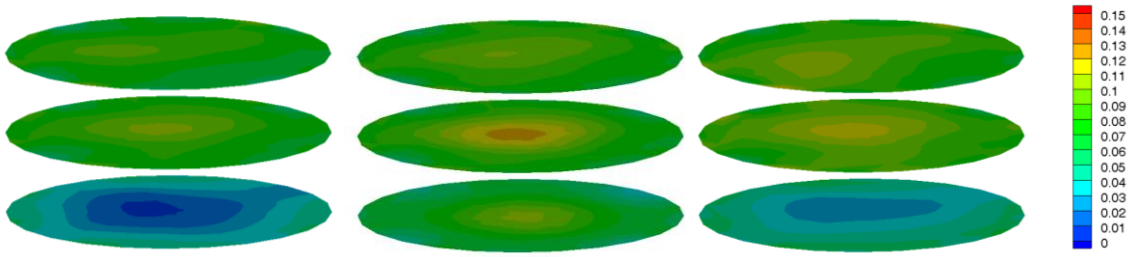


*(a)* *(b)* *(c)*

*Figure 3: Gas volume fraction on the three ERT planes. (a) $Q_G$=50 L/min, N=250rpm; (b) $Q_G$=50 L/min, N=315rpm; (c) $Q_G$=120 L/min, N=250rpm.*

For a stricter quantitative evaluation of the gas volume fraction at the different locations, selected radial profiles of azimuthally averaged gas volume fraction, as extracted from the maps of Figure 3(a) and (b) are reported in Figure 4. The profiles showed that with the increase of the impeller speed from 250 to 315 rpm the bubbles are pumped below the lower impeller, thus moving from loading to complete dispersed conditions. It is worth observing that due to the limited optical access of the system, the ERT measurements are particularly useful for estimating the expected mass transfer performances of stirred bioreactors working in similar conditions.

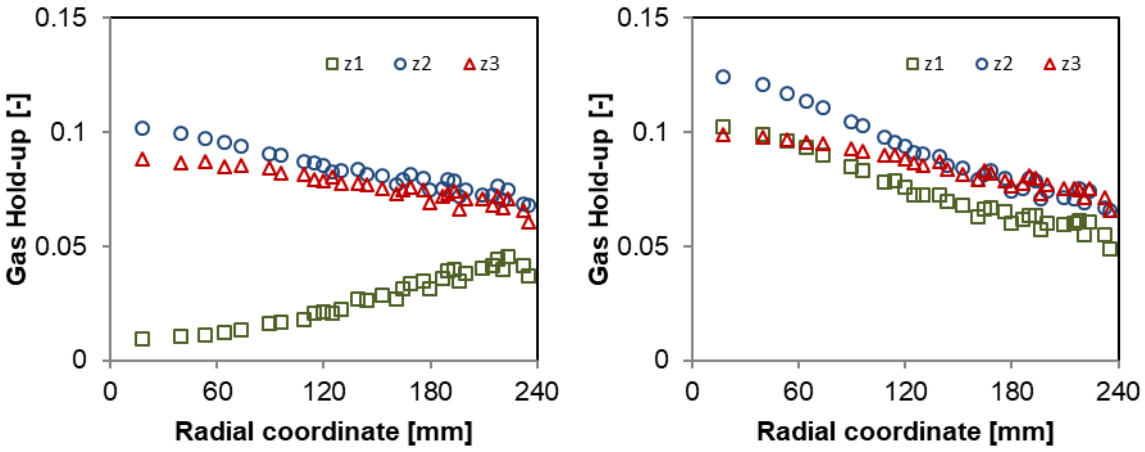


*(a)* *(b)*

*Figure 4: Azimuthally averaged radial profiles of gas volume fraction on the three ERT planes (a) $Q_G$=50 L/min and N=250rpm. (b) $Q_G$=50 L/min and N=315rpm*

The ERT measurements also allow the monitoring of the transient behaviour of the system. From the time trace of the plane averaged dimensionless conductivity shown in Figure 5, the conductivity on the three planes during the aeration starting from the ungassed liquid takes hundreds of seconds to achieve a steady distribution. As soon as the aeration is switched off, the conductivity exhibits unphysical values, most likely due to the isolation of some of the electrodes due to the bubble passage. Afterwards, the conductivity trend provides an indication of the bubble rise velocity, which is of interest when the direct measurement of the bubble size is not possible.

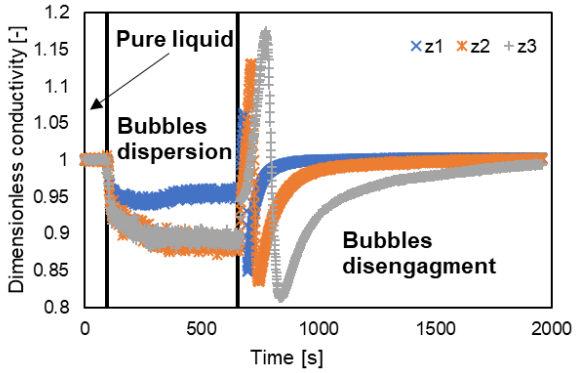


*Figure 5: Time trace of dimensionless conductivity in the stirred tank starting from the ungassed condition until the total gas disengagement after stopping the aeration, $Q_G$=50L/min e N=250rpm.*

Figure 6 shows an example of the Bubble size distribution measured with the Malvern Spraytec. In all the experiments, practically, the bubbles can be assumed as monodispersed.

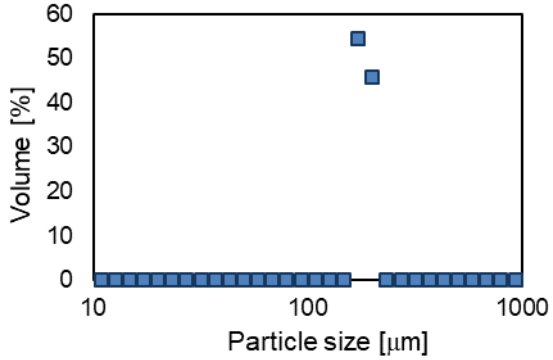


*Figure 6: Bubble size distribution, $Q_G$=120 L/min and N=315rpm*.

The bubble Sauter diameter is shown in Figure 7(a) as a function of the gas flow number, defined as the ratio between the gas flow rate and $ND^3$. As can be observed, it is much smaller than in water-air dispersions in stirred tanks in similar operative conditions, typically of a few mm, due to the low surface tension of the liquid with respect to water. It exhibits an increase of about 30μm around the gas flow number of 0.03, which is most likely due to a decrease of the breakage rate.

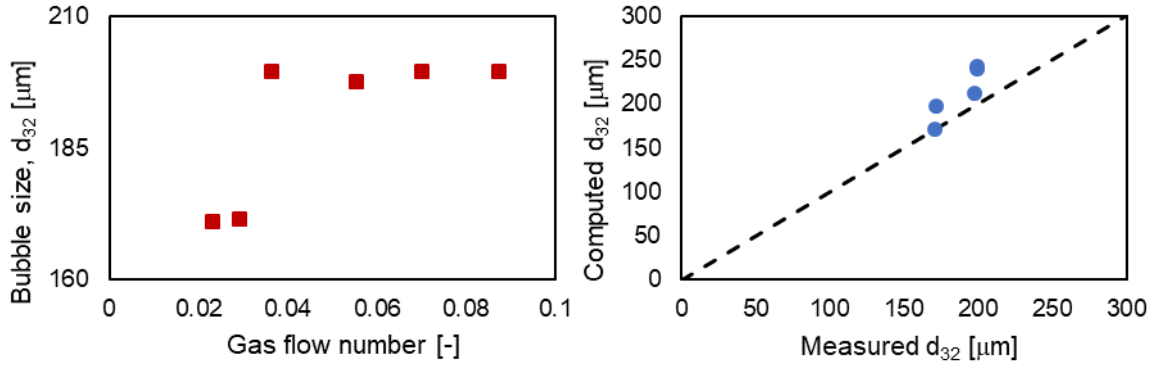


*(a)* *(b)*

*Figure 7: Bubble Sauter diameter at different gas flow number (a) and comparison between estimated and measured values (b).*

From the bubble rise velocity, obtained from the cross-correlation of the conductivity time traces shown in Figure 5, it is possible to calculate the bubble size, from the force balance on a single bubble and a suitable drag

coefficient correlation. In the present work, the drag coefficient has been estimated using the Schiller and Nauman correlation, since in the investigated conditions the bubbles can be approximated to rigid spheres (Maluta et al., 2021). The calculated and the measured bubble sizes are in fair agreement, as it is shown in Figure 7(b). These results suggest a promising possibility to extract bubble rise velocity and size from the ERT data, which will be further explored in future investigations.

## 4. Conclusions

The effectiveness of a SAFD in an aerated dual impeller stirred tank working with a liquid exhibiting a foaming behaviour similar to many fermentation broths is assessed. The up-pumping SAFD was proved to be reliable in all the operative conditions considered. Operative conditions for ensuring uniformity of gas distribution, acceptable power consumption and narrow bubble size distribution for mass transfer optimization can be identified by combining ERT, Laser diffraction and strain gauge instrumentation without direct optical access in the vessel. Future work will be devoted to the identification of an optimized set-up able to guarantee high values of the specific surface area in the liquid phase, required in the gas/liquid mass transfer processes, limiting the foam formation in the headspace.

### References

Boon L.A., Hoeks F.W.J.M.M., Van Der Lans R.G.J.M., Bujalski W., Wolff M.O., Nienow A.W. 2002, Comparing a range of impellers for "stirring as foam disruption", Biochemical Engineering Journal, 10, 183-195. DOI: 10.1016/S1369-703X(01)00180-2.

Carletti C., Bikic S., Montante G., Paglianti A., 2018, Mass transfer in dilute solid−liquid stirred tanks, Industrial and Engineering Chemistry Research, 57, pp. 6505 – 6515. DOI: 10.1021/acs.iecr.7b04730.

Falzone S., Buffo A., Vanni M., Marchisio D.L., 2018, Simulation of Turbulent Coalescence and Breakage of Bubbles and Droplets in the Presence of Surfactants, Salts, and Contaminants, Advances in Chemical Engineering, 52, 125 - 188. DOI: 10.1016/bs.ache.2018.01.002.

Hoeks F.W.J.M.M., Boon L.A., Studer F., Wolff M.O., Van Der Schot F., Vrabél P., Van Der Lans R.G.J.M., Bujalski W., Manelius Å., Blomsten G., Hjorth S., Prada G., Luyben K.Ch.A.M., Nienow A.W., 2003, Scale-up of stirring as foam disruption (SAFD) to industrial scale, Journal of Industrial Microbiology and Biotechnology, 30, 118 - 128. DOI: 10.1007/s10295-003-0023-7.

Hoeks W.J.M.M.F., Van Wees-Tangerman C., Gasser K., Mommers H.M., Schmid S., Luyben K.Ch.A.M., 1997, Stirring as Foam Disruption (SAFD) Technique in Fermentation Processes, Canadian Journal of Chemical Engineering, 75, 1018 - 1029. DOI: 10.1002/cjce.5450750604.

Jiang, J., Zu, Y., Li, X., Meng, Q., Long, X., 2020, Recent progress towards industrial rhamnolipids fermentation: Process optimization and foam control, Bioresource Technology, 298, art. no. 122394. DOI: 10.1016/j.biortech.2019.122394.

Junker B., 2007, Foam and its mitigation in fermentation systems, Biotechnology Progress, 23, 767 - 784. DOI: 10.1021/bp070032r.

Khalili, F., Jafari Nasr, M.R., Kazemzadeh, A., Ein-Mozaffari, F., 2017. Hydrodynamic performance of the ASI impeller in an aerated bioreactor containing the biopolymer solution through tomography and CFD. Chem. Eng. Res. Des. 125, 190-203. https://doi.org/10.1016/j.cherd.2017.07.016.

Leuner, H., Gerstenberg, C., Lechner, K., McHardy, C., Rauh, C., Repke, J.-U., 2020, Overcoming unwanted foam in industrial processes of the chemical and food industry – an ongoing survey, Chemical Engineering Research and Design, 163, 281-294. DOI: 10.1016/j.cherd.2020.09.006.

Maluta F., Paglianti A., Montante G., 2021, Prediction of gas cavities size and structure and their effect on the power consumption in a gas-liquid stirred tank by means of a two-fluid RANS model, Chemical Engineering Science, 241, art. no. 116677. DOI: 10.1016/j.ces.2021.116677.

Maniscalco F., Raponi A., Vanni M., Buffo A., 2021, Computational modeling of the impact of solid particles on the gas hold-up in slurry bubble columns, Chemical Engineering Transactions, 86, pp. 1141 - 1146. DOI: 10.3303/CET2186191.

Montante G., Paglianti A., 2015, Fluid dynamics characterization of a stirred model bio-methanation digester, Chemical Engineering Research and Design, 93, pp. 38 - 47. DOI: 10.1016/j.cherd.2014.05.003.

Montante G., Magelli F., Paglianti A., 2013, Fluid-dynamics characteristics of a vortex-ingesting stirred tank for biohydrogen production, Chemical Engineering Research and Design, 91, 2198 – 2208. DOI: 10.1016/j.cherd.2013.04.008.

Varley J., Brown A.K., Boyd J.W.R., Dodd P.W., Gallagher S., 2004, Dynamic multi-point measurement of foam behaviour for a continuous fermentation over a range of key process variables, Biochemical Engineering Journal, 20, 61 - 72. DOI: 10.1016/j.bej.2004.02.012.